OUKA
The University of Osaka
Institutional Knowledge Archive

Title	Some Properties of 30KW-Class Electron Beam for Welding
Author(s)	Arata, Yoshiaki; Tomie, Michio; Kato, Yutaka
Citation	Transactions of JWRI. 1973, 2(1), p. 7-15
Version Type	VoR
URL	https://doi.org/10.18910/8688
rights	
Note	

The University of Osaka Institutional Knowledge Archive : OUKA

https://ir.library.osaka-u.ac.jp/

The University of Osaka

Some Properties of 30 KW-Class Electron Beam for Welding†

Yoshiaki ARATA*, Michio TOMIE** and Yutaka KATO***

Abstract

The material properties and the life time of thermionic emission type cathode which generates high power electron beam is discussed. Properties of weld bead penetration using the 30~150KV electron beam are investigated and the empirical formula for the penetration depth is introduced. Ion beam, produced by the electron beam and passing through the accelerating space of an electron beam gun, is measured, and also its properties are discussed.

1. Introduction

The cathode is one of the most important part of an electron beam gun and determines its capability. As desired such a thermionic emission type cathode of the high power electron beam gun can emit a large stable quantity of thermoelectrons for many hours.

The accelerating space of the welding electron beam gun is usually tainted by environment gases and "welding vapors" (which evaporate from the welded metal during welding). The spattering of the chathode material, caused by impact of ion beam produced by electron beam, is remarkable and it makes the cathode life time shorter. Then, concerning the material, the shape and the location of the cathode, many attempts or devices have been made but there is no definite conclusion. In this report. Tungsten (W) and Tantalum (Ta) were selected and discussed as the cathode material which stably generates welding high power electron beam for many hours.

Using the EB-welder with electron beam gun which was developed by the authors, the bead penetration test was carried out against SUS304 stainless steel which corresponds with AISI304 and the emprical formula for the penetration depth was introduced.

2. Experimental Apparatus and Materials

For the experimental apparatus, the following two types of EB-welders developed by authors were used.

A type: V_b=50~150[KV], I_b=0~50[mA], W_b=7.5[KW]

B type: V_b=30~60[KV], I_b=0~500[mA], W_b=30[KW]

where V_b[KV] is an accelerating voltage of electron beam, I_b[mA] is the electron beam current and W_b [KW] is the maximum beam power.

Figure 1 shows a principle drawing of electron beam gun and beam channel in case that the work chamber can be utilized up to 10^{-1} from 10^{-4} Torr.

Figure 2 shows a circuit diagram.

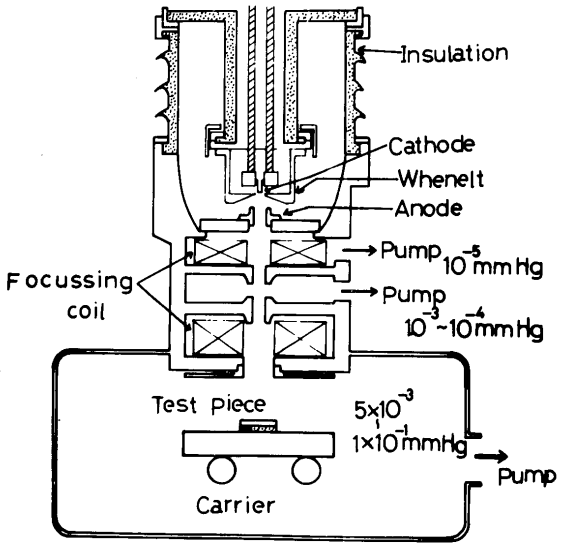

Fig. 1. Schematic diagram of EB-welder.

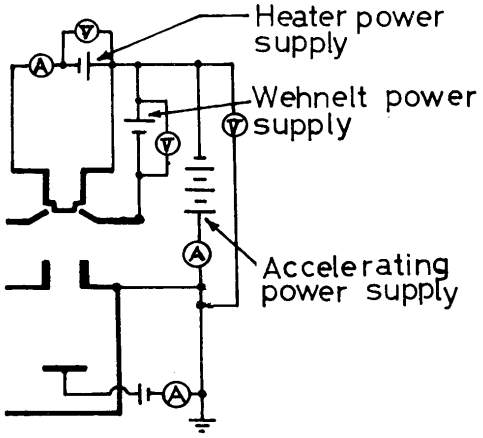

Fig. 2. Circuit diagram of EB-welder.

† Received on Nov., 25, 1972

* Professor
** Research Associate
*** Research Associate, Iron and Steel Technical College

The electron beam gun is a Pierce type and the open angle of whennelt is 90° and its open diameter is 6.5 mmϕ. SUS304 type stainless steel was used as the experimental material.

3. Results and Discussions

3.1 Cathode Materials

As it is well known, the following formula has been obtained. Concerning the properties of the thermionic emission type cathode material.

$$\left.\begin{array}{ll} \text{thermionic emission}^{1)}: & i_{th} \propto e^{-V_W/V_T}, \left\{\dfrac{\text{Amp}}{\text{cm}^2}\right\} \quad \text{.....(a)} \\ \text{evaporation}^{2)} & : M_{vap}=5.83\times10^{-2}p\sqrt{\dfrac{M}{T}}, \\ & \left\{\dfrac{\text{g}}{\text{cm}^2\cdot\text{sec}}\right\} \text{.....(b)} \\ \text{evaporation rate} & : v_{vap}=\dfrac{M_{vap}}{\rho}, \left\{\dfrac{\text{cm}}{\text{sec}}\right\} \text{..... (c)} \end{array}\right\} \text{(1)}$$

where T[°K] and V_T [volt] indicate the temperature of the cathode material, and V_W [volt], ρ[g/cm^3], p and M are its work function, density, vapor pressure and molecular mass per grams respectively.

The formula (a) shows higher density thermoelectron flow is obtained by the material of higher V_T value and lower V_W value. The pure materials which can elevate the V_T value are high melting point materials, W, Re, Ta and Mo in order, and Ta, Mo, W and Re are in order of lower V_W value. It can be noticed that Mo is inferior to Ta on both the above properties, and it is better to discuss for W, Ta and Re.

Figures 3 and **4**[3) 4)] illustrate the formula (1). Although the formula (b) and (c) are related to the life time, the formula (c) is more convenient compared with the formula (b). From these, it can be noticed that Ta is somewhat better compared with Re as the cathode material at each temperature in practical continuous usage. Moreover, Ta has more advantages over W in the manufacturing property. Therefore it seems that Ta is the best conthode material. But it is necessary to take some considerations as follows that is the accelerating chamber in the EB-welder is usually tainted and damaged by environmental gases and welding vapors. Especially, ions, produced by electron beam, are accelerated as ion beam to the opposite direction against electron beam in the accelerating chamber, impact with the cathode material and damage it. This is named "ion beam etching" or simply "beam etching". The effect of the beam etching is stronger than any other mechanism and not only makes the cathode life time short. But it damages both the stability of the electron beam power and the beam focusing. Resistance of Ta against the beam etching is inferior to W resistance.

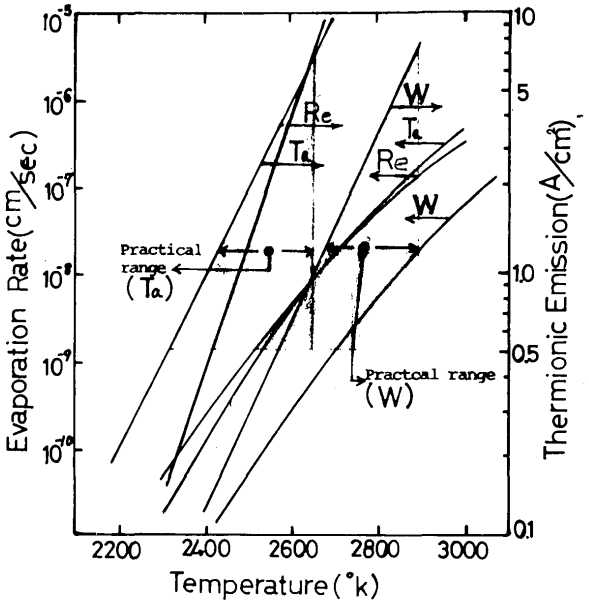

Fig. 3. Relation of evaporation rate, thermionic emission and cathode temperature.

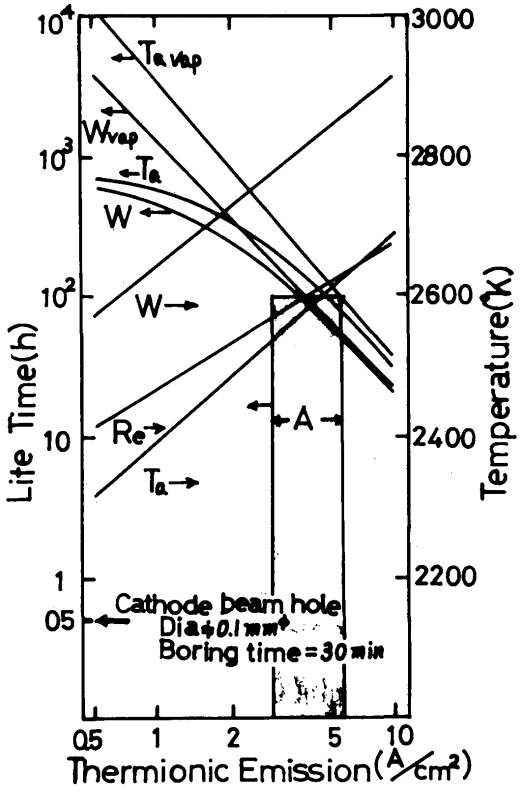

Fig. 4. Relation of life time, temperature and thermionic emission for the cathode.
(A: Range used generating electron beam for 100 hours)

Futhermore, required properties of the cathode material are that the mechanical strength is high and both expansion and contraction are small in the

region of service temperature. In case of the large coefficient of expansion or construction, the cathode is deformed and its fitting position is away from the original position; consequently, it is difficult to generate a stable electron beam. And in case of the low mechanical strength at the service temperature, the cathode material is apt to be deformed or to be destroyed by electromagnetic force, generated from the large electric current heating the cathode material, consequently, stable electron beam is difficult to obtain.

W is superior to Ta against both properties of the mechanical strength and the coeffiecient of expansion at each practical service temperature as shown in **Fig. 5.**[5), 6)]

For example, the cathode materials of W and Ta must be heated up to 2700°K and 2500°K respectively in order to obtain i_{th}=2 A/cm^2 as the beam current density, but in this case, the fracture strength of W is 4[Kg/mm^2] and the strength of Ta is 1.8[Kg/mm^2], consequently, W is 2.2 times fracture strength of Ta. Futher, the coefficients of expansion of W and Ta are 6.9 and 10.1 respectively. From these, it seems that W has the most suitable properties as the cathode material of high power welding beam gun. So we used it for our developed powerful welding guns.

So far various shapes of the cathode mater have been used. The typical shapes are hair-pin type, square type (square, rectangle), spherical winding type and circle type. Circle type showed the best beam property among these types, so we used the circle type, 3 mm in diameter.

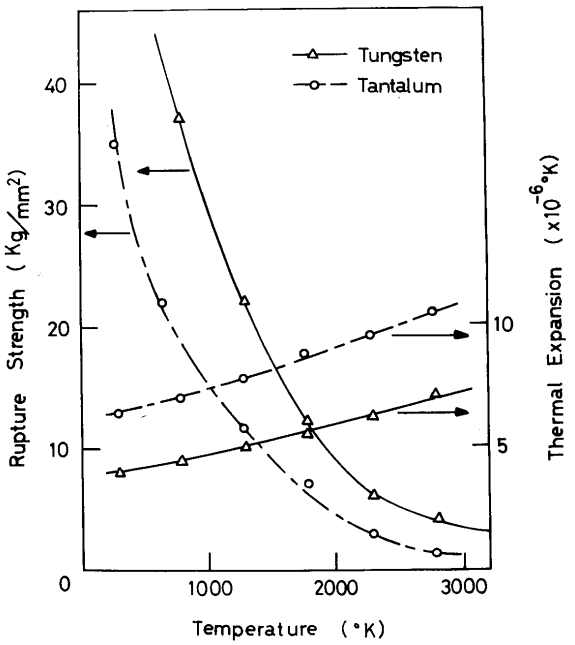

Fig. 5. Relation of rupture strength, thermal expansion and cathode temperature for W and Ta.

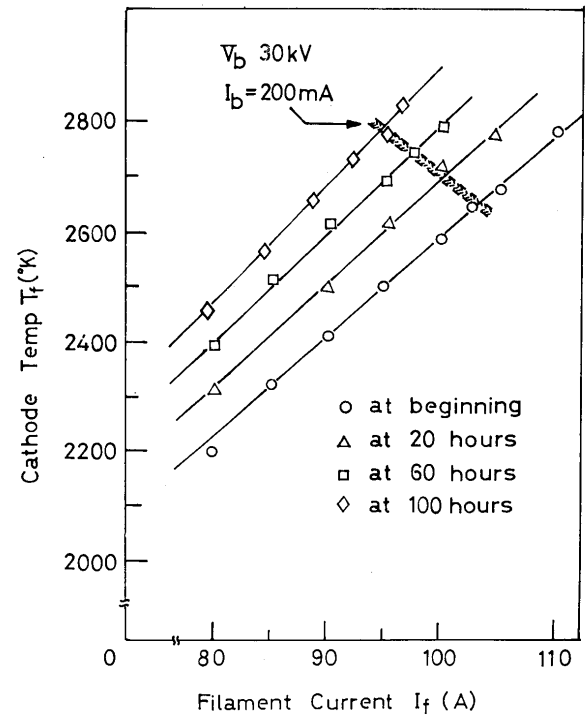

Fig. 6. Relation of cathode temperature and filament current keeping constant; V_b=30 KV, I_b=200 mA.

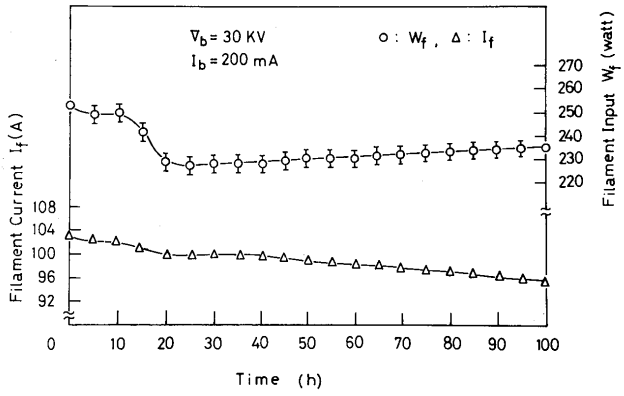

Fig. 7. Relation of filament current, input power and time. keeping constant; V_b=30 KV, I_b=200 mA.

Figure 6 shows I_f-T_f characteristic curve and **Fig. 7** is characteristic curve of I_f-T_f-time, where I_f is an electric current heating the cathode, that is, filament current, T_f is temperature of cathode material heated with I_f and W_f is input power required to heat the cathode material. As shown in these figure, in case that I_b=200 mA was taken out for 100 Hr. continuously, I_f decreased gradually from 103[A] to 97 [A].

Also, small decreases on W_f and I_f were recognized after 10~20 min operation, and they remarkably decrease after 15~20 hours. This phenomenon occurs when the center of cathode material is remarkably consumed by beam etching, caused by above-mentioned ion beam. Consequently, boring

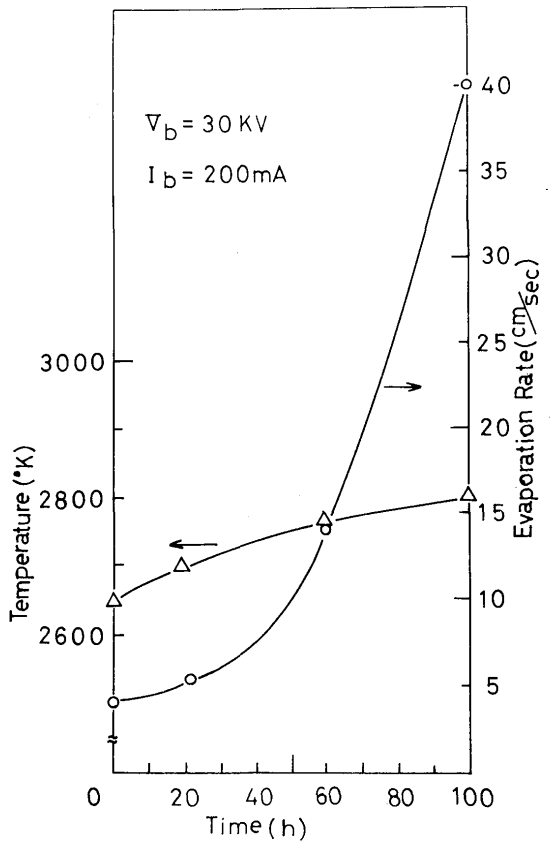

Fig. 8. Relation of cathode temperature, evaporation rate and time. keeping constant; V_b=30 KV, I_b=200 mA.

Table 1. One example of consumption rate of cathode.

Location / Thickness (mm)	A	B	C	D	E
t_0 (before use)	0.177	0.179	0.174	0.174	0.176
t_{100} (after use)	0.150	0.157	0.153	0.143	0
$\Delta t = (t_0 - t_{100})$	0.027	0.022	0.021	0.031	0.176

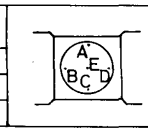

phenomenon is caused and the effective area of the cathode decreases. After that, their curves gradually change. It seems that these phenomena are caused by a continuous decrease of the valume of the cathode material, based on the various mechanisms as shown in **Fig. 8** and **Table 1.**

3.2 Ion Beam

It is known that the high density beam plasma is produced by the powerful electron beam at the suitable gas pressure, $P_{ch} \gtrsim 10^{-4}$ Torr.[7]

During welding, in general, such condition of the gas pressure is fully satisfied in a work chamber and the high density beam plasma is practically formed as shown in **Fig. 9.**[8]

Ions among the beam plasma are caught by electron beam itself and the ion motion drifting away from the beam axis is restrained. On the contrary, the drift along the beam axis is easy.

The ions are accelerated to the opposite direction of electron beam by receiving the same accelerating voltage as the electron beam in the accelerating space and impact strongly with the cathode material as ion beam. Such ion beam can be divided into "concentrated ion beam" which is constricted near the electron beam axis and "distributed ion beam" which is distributed widely over the beam plasma region. The former is high density and causes the violent beam etching accompanying the strong boring phenomenon against the cathode material. and the latter is low density and makes gradually the consumes the whole cathode.

Figure 10 illustrates schematically an aspect of their distribution when electron beam of I_b=200 mA is emitted into the work chamber with $P_{ch}=6\times10^{-5}$ Torr,

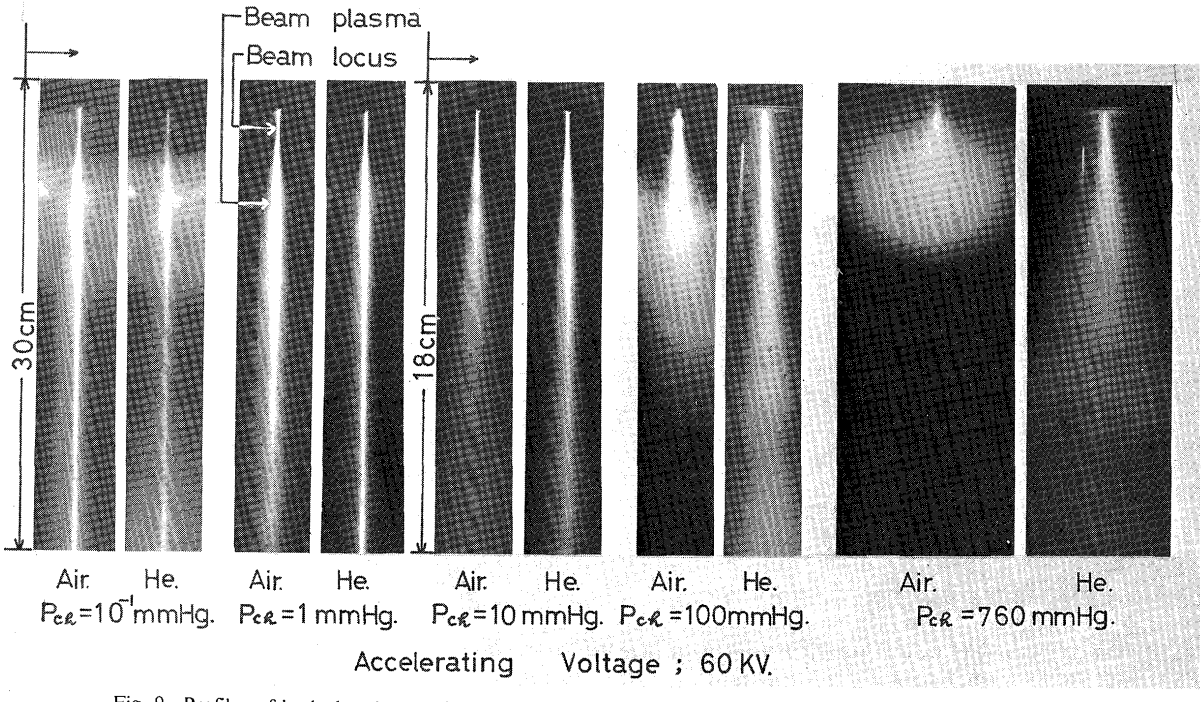

Fig. 9. Profiles of both the electron beam and beam plasma against various gas pressures (P_{ch}).

by using the electron beam gun with beam perveance of $G_b=2.3\times10^{-8}$, and W-cathode of 0.15 mm in thickness, is fully penetrated by concentrated ion beam after 24 min. as shown in **Fig. 11.** Further, after 20 houres, this small hole, cathode beam hole with about 1.0 mm in diameter, is formed as shown in **Fig. 12 (a).**

As a result, beam etching speed (v_{etch}=cathode material thickness/penetration time) in this case is nearly $v_{etch}\fallingdotseq1\times10^{-5}$ cm/sec and the forming time of the cathode beam hole is 24 min. Therefore it can be considered that average diameter of the concentrated ion beam is nearly same, 1.0 mmϕ in this case, as this

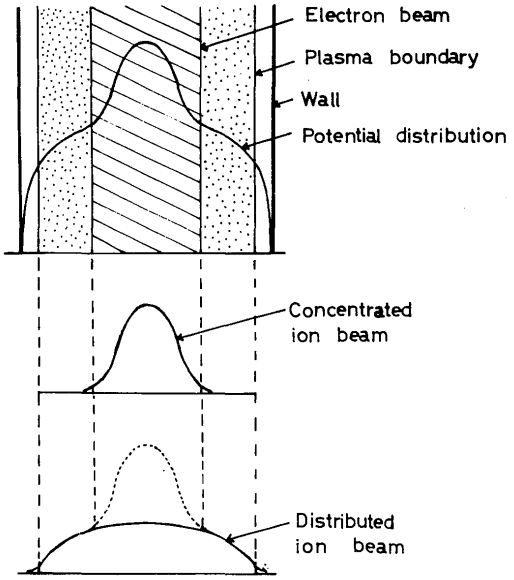

Fig. 10. Schematic distribution of both concentrated and distributed ion beam.

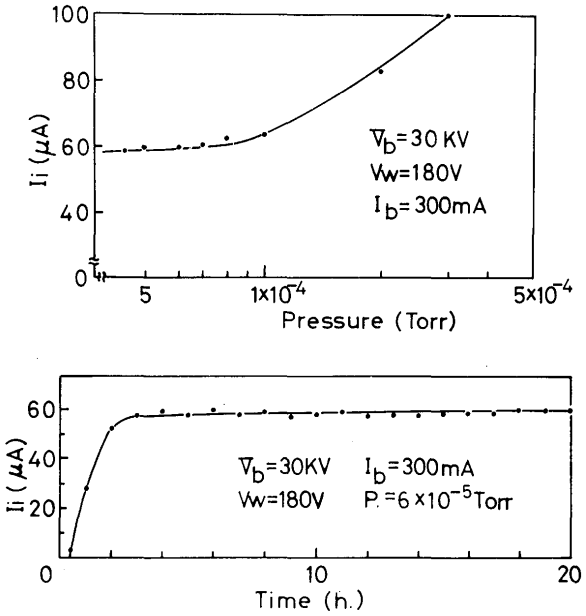

Fig. 11. Ion beam current against gas pressure in gun and elapsed time. (Ion beam appears suddenly after a certain times elapsed 24 min, due to full penetration). V_w (=180 V) is wehnelt voltage.

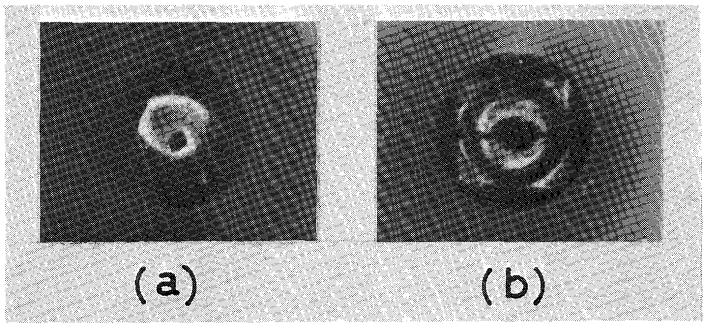

Fig. 12. Examples of beam etching against the cathode (a; V_b=30 KV, I_b=300 mA, Time=after 20 hours. b; V_b=30 KV, I_b=400 mA, Time=after 76 hours.)

cathode beam hole, and also cathode beam hole with 2.0 mmϕ is bored after 76 hours as shown in **Fig. 12 (b).**

Beam etching property is, namely, that its action concentrates near the center of the cathode in the same range as concentrated ion beam diameter and makes the cathode beam hole in a short time, and the circumference is gradually etched by the distributed ion beam. **Figure 13** shows a principle drawing of measuring apparatus of concentrated ion beam and **Fig. 11** shows the measured results and it was recognized that concentrated ion beam current was about 60 μA under such conditions that V_b=30 KV, I_b =300 mA, $P_{ch}=6\times10^{-5}$ Torr.

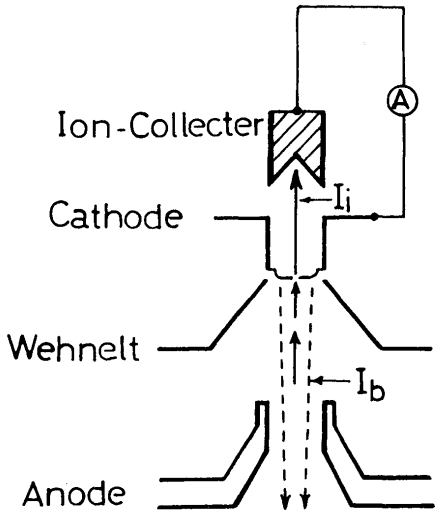

Fig. 13. Measuring method of concentrated ion beam.

3.3 Welding Bead Penetration

Although so far many papers[9), 10), 11)] were presented to search the mechanism of welding bead penetration, these are not treated systematically. General formula on the penetration depth, h_p, has been given by one of authors[12)] as follows.

$$h = K\, h(s)\, h(\varepsilon) \qquad (2)$$

$$\text{where, } h(s)=f(a_b\cdot l_b\cdot \theta_b\cdot \theta_s) \quad \text{---------- (a)}$$
$$h(\varepsilon)=f(W_b\cdot w_b\cdot v_b) \quad \text{---------- (b)} \qquad (3)$$

now, we will let

$$h(\varepsilon)=\frac{W_b^{n_1}\, w_b^{n_2}}{v_b^{n_3}} \quad \text{---------- (a)}$$
$$=\frac{I_b^{m_1}\, V_b^{m_2}}{v_b^{m_3}\, d_b^{m_4}} \quad \text{---------- (b)} \qquad (4)$$
$$=\frac{I_b^{l_1}\, V_b^{l_2}}{v_b^{l_3}} \quad \text{----------(c)}$$

h(s) and h(ε) are called "beam shape function" and "beam energy function" respectively, because h(s) and h(ε) indicate the degree of each action of the beam shape and the beam energy for the penetration. **Fig. 10** is one example illustrating the positive influence of h (s) on the penetration.

K is a constant of welding materials and a_b, l_b, θ_b and θ_s are "beam active parameter"(active parameter), length of "beam active zone", beam convergent angle and angle of slope welding respectively as shown in **Fig. 14** and **Fig. 15.** n_1, n_2, and n_3 are parameters which show the degree of the effects of beam power, W_b, beam power density, w_b, and welding speed, v_b, on penetration respectively. m_1, m_2, m_3 and m_4 are parameters which show the degree of the effects of I_b, V_b, v_b and d_b (beam diameter) on the penetration respectively. Accordingly, under such condition that h(s) maximize h_p, formula (4), (c) is adopted to obtain the most simple empirical formula for h(ε). In this case, we will let

$$K_m=K\{h(s)\}_{h_p=\max} \quad \text{---------- (5)}$$

It is considered that K_m value depends on the sort of the welding materials and the EB-welders (which differentiate in characteristics of the welding beam gun), because h(s) depends on the EB-welder in general. Then using the given EB-welder and such condition that h(s) maximize h_p for the given materials, K_m is constant.

Then using formulas (4), (c) and (5), formula (2) is as follows.

$$h_p=K_m\, h(\varepsilon)=K_m\frac{I_b^{l_1}\, V_b^{l_2}}{v_b^{l_3}} \quad \text{---------- (6)}$$

To obtain K_m, l_1, l_2, and l_3 in formula (6), the relation of h_p against I_b, V_b and v_b was obtained experimentally for SUS304 stainless steel under a variety of welding conditions. The results are shown in **Figs. 16 ~21.**

As a result. as it is obtained for both A type and

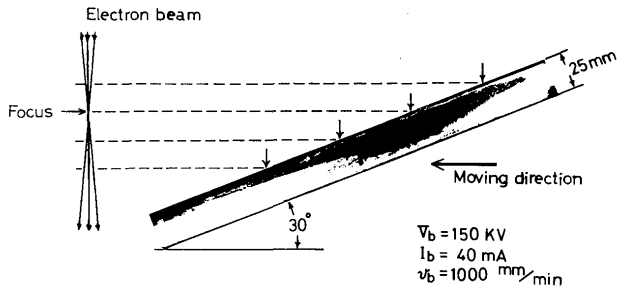

Fig. 14. Example of slope welding.

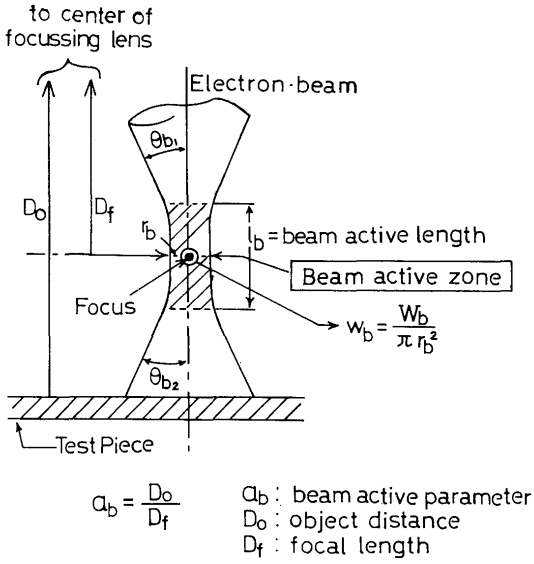

Fig. 15. Schematic diagram illustrated both shape of electron beam and many beam parameters.

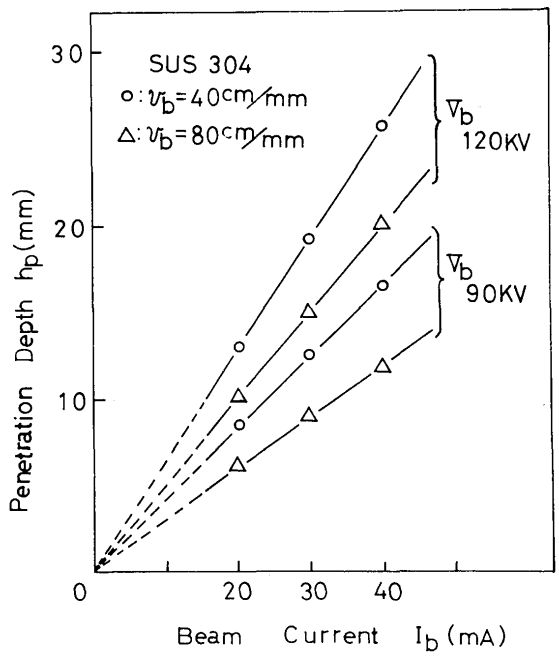

Fig. 16. I_b-h_p relation; A type-EB apparatus. (SUS304 correspond to SUS27 or AISI304)

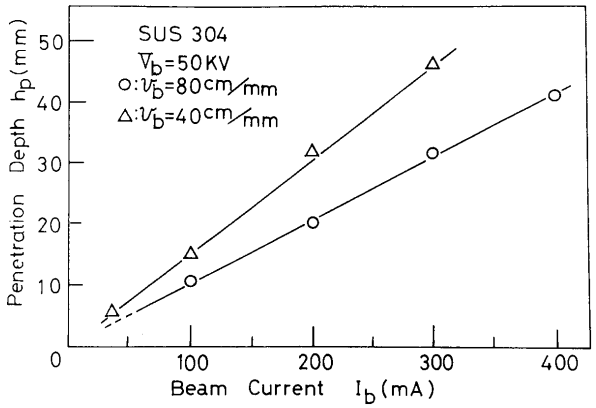

Fig. 17. I_b-h_p relation; B type-EB apparatus.

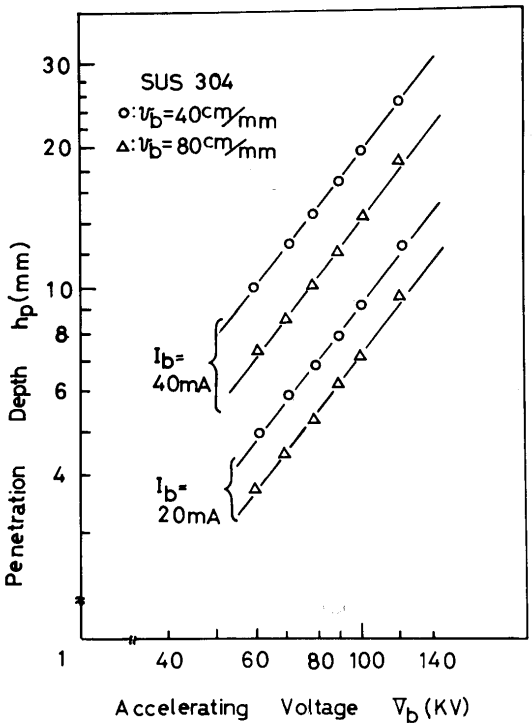

Fig. 18. V_b-h_p relation; A type-EB apparatus.

B type that l_1=1, l_2=1.3 and l_3=0.5, the following formula establishes within experimented range.

$$h(\varepsilon) = \frac{I_b\ V_b^{1.3}}{v_b^{0.5}} \quad \text{---------- (7)}$$

As described above, it is also proved in eq (7) that K_m depends on both of the materials and EB-welders. Then using EB-welders of A type and B type for SUS-304 stainless steel, it was obtained such as $K_m=7.93\times10^{-3}$ and 5.51×10^{-3} respectively.

Therefore the empirical formula of h_p becomes as follows.

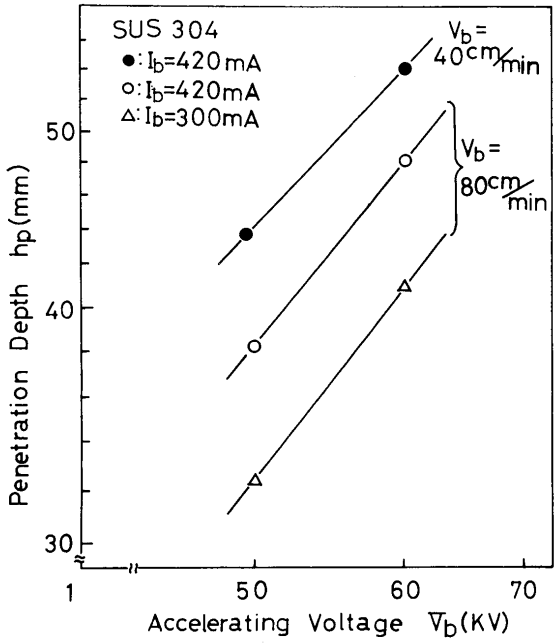

Fig. 19. V_b-h_p relation; B type-EB apparatus.

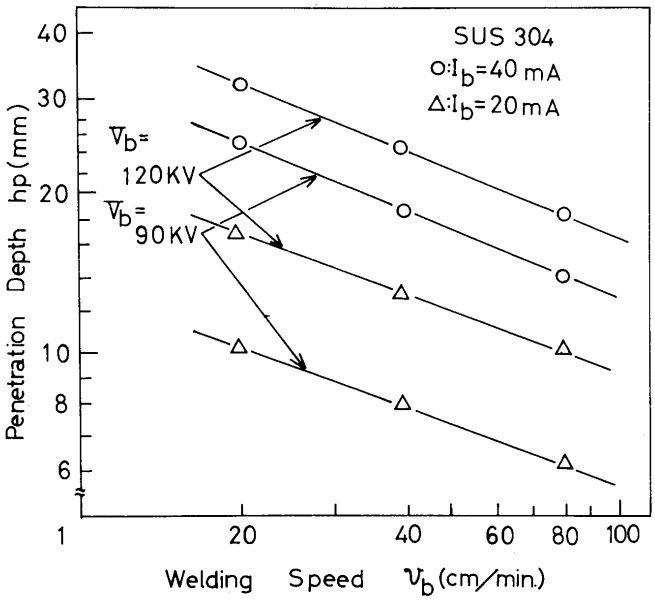

Fig. 20. v_p-h_p relation; A type-EB apparatus.

$$\left.\begin{aligned} h_p &= 7.93\times10^{-3}\ \frac{I_b\ V_b^{1.3}}{v_b^{0.5}} \quad \text{(A type) --------- (a)} \\ &= 5.51\times10^{-3}\ \frac{I_b\ V_b^{1.3}}{v_b^{0.5}} \quad \text{(B type) ---------- (b)} \end{aligned}\right\} \quad (8)$$

Figure 22 shows the relation between calculated value from formula (8), (a) and measured value, and it shows close agreement. Also the calculated result from formula (8), (b) agrees well with the measured value as shown in **Fig. 23.**

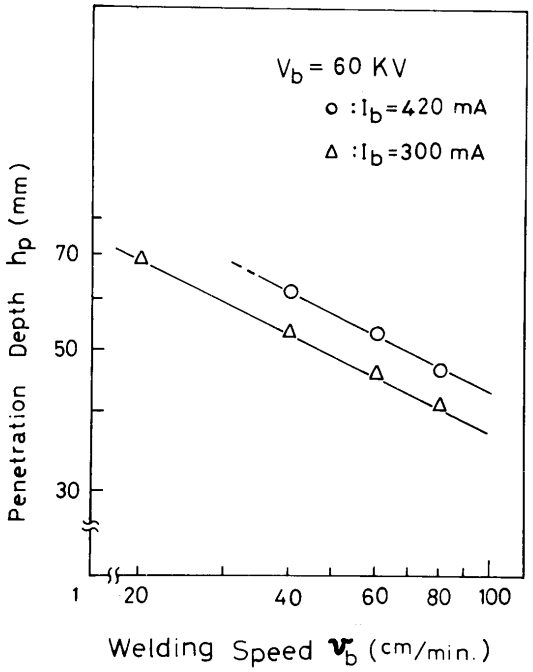

Fig. 21. v_b-h_p relation; B type-EB apparatus.

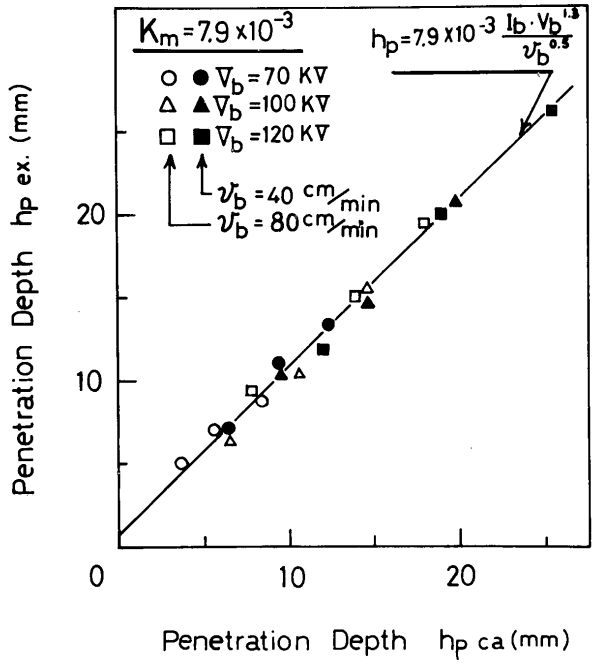

Fig. 22. Correlation between calculated penetration depth and actual depth in case of A type apparatus.

However it is noticed that formulas (6) and (8) can only apply within a region K_{v1} K_{v2} where h_p is almost proportional against $1/\sqrt{v_b}$ as shown in **Fig. 24** ,moreover $K_{v1} \fallingdotseq 0.05$ and $K_{v2} \fallingdotseq 0.2$ are obtained in case of SUS304, without regard to the change of weld conditions in most cases. We introduce general formula which can apply in more wide range covered all over the experimented region as shown in **Fig. 24.** We see that

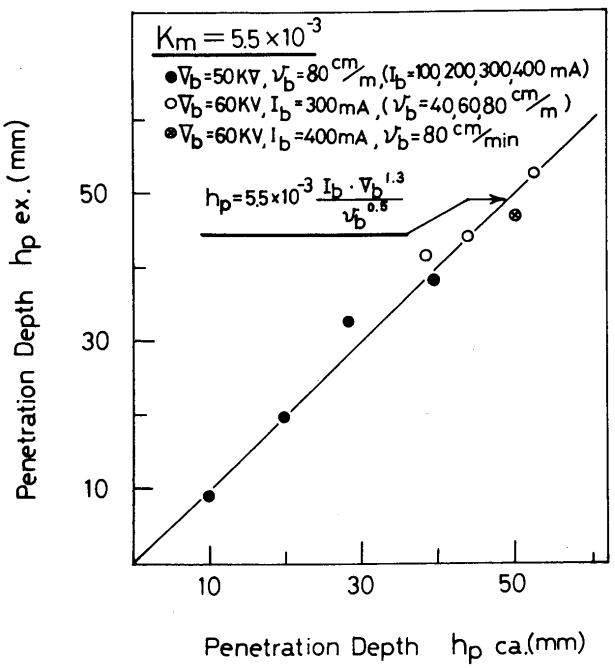

Fig. 23. Correlation between calculated penetration depth and actual depth in case of B type apparatus.

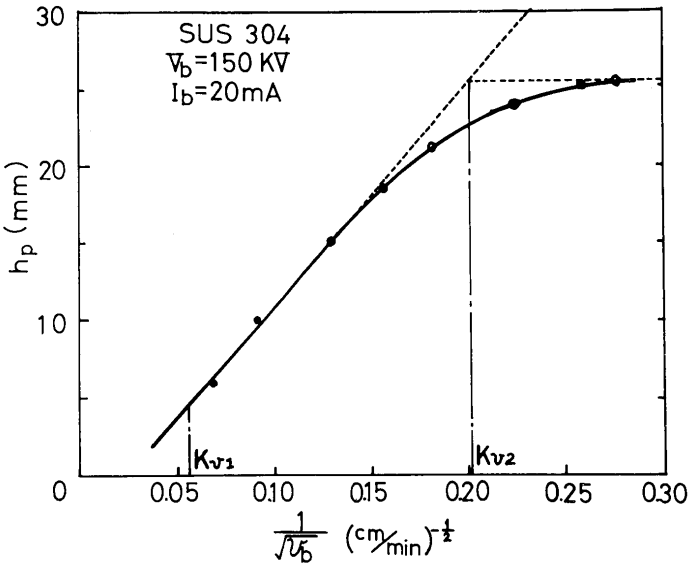

Fig. 24. Relations between h_p and $\frac{1}{\sqrt{v_b}}$

$$h_p = h_{p0}(1-e^{-\frac{K_0}{v_b^l}}) \quad \text{---------- (9)}$$

Where h_{p0} is h_p in $v_b=0$, K_0 and l are constant. If v_b becames large ($1/v_b^l$ is small) and $K_0/v_b^l \ll 1$ in formula (9), we see that

$$\left.\begin{aligned} h_p &= h_{p0}\{1-\{1+(-\frac{K_0}{v_b^l}) + \frac{1}{2!}(-\frac{K_0}{v_b^l})^2 \\ &\quad + \frac{1}{3!}(-\frac{K_0}{v_b^l})^3 + \cdots\}\} \quad \text{----- (a)} \\ &\fallingdotseq h_{p0}\{1-(1-\frac{K_0}{v_b^l})\} = \frac{K\, h_{p0}}{v_b^l} \quad \text{--------- (b)} \end{aligned}\right\} \text{--- (10)}$$

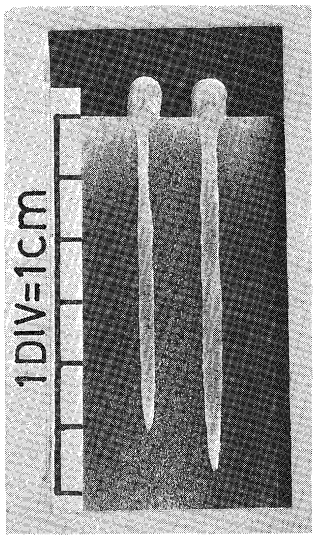

Fig. 25. Bead section at maximum penetration using B type EB-welder (left side ; I_b=320 mA, V_b=60 KV, v_b=40 cm/min, right side; I_b=420 mA, V_b=60 KV, v_b=40 cm/min)

Here, letting l=0.5, it is recognized that approxmate formula (10), (b) agrees with (6) or (8).

Figure 25 shows the respective typical bead section photographs at max. penetration part in case that I_b=420 mA and 320 mA against V_b=60 KV and v_b=40cm/min using B type EB-welder.

4. Conclusion

Obtained conclusion is as follows:

1) It was expressed that tungsten, W, is superior as cathode material of the powerful welding electron beam gun.
2) W-cathode properties of circle type were investigated and it was shown that the cathode of 30 KW-class electron beam gun which has the life time over 100 Hr. can be obtained.
3) Ion beam properties in an electron beam gun were discribed and beam etching action of the ion beam for cathode material was investigated.
4) General formulas for welding penetration using powerful electron beam up to 30 KW-class were given and the emprical formulas were introduced.

Acknowledgment

The authors thank Dr. Matsuda and Mr. Inoue for their discussions.

References

1) S. Dushman: "Electron Emission from Metals as a Function of Temperature", Phys. Rev. 21 (1923).
2) S. Dushman: "Scientific Foundation of Vacuum Technique", 2nd ed. Wiley., New York (1962).
3) R. N. Bloomer: Prc. IEE., 104 B, March (1957).
4) O. S. Heavens: Proc. Phys. Soc. B., 65 (394), (1952).
5) E. N. Marmer et al "High Temperature Materials", (Trans. in Japanese) Publishing House "Metallurgy", (1967).
6) R. S. Hernicz and R. L. Feng: "Thermophysical Properties of High Temperature Solid Materials", Y. S. Touloukian, Ed., Vol. 1, Thermophysical Properties Research Center, Purdur Univ., (1967).
7) P. Hedvall: Jour. Appl. Phys. 33 (1962).
8) Y. Arata and M. Tomie: "Some Fundamental Properties of Nonvacuum Electron Beam", Trans. Japan Welding Society, Vol. 1 No. 2 (1970).
9) T. Hashimoto and F. Matsuda: "Effect of Welding Variables and Materials upon Bead Shape in Electron Beam Welding", Trans. National Institute Metals, Vol. 7 No. 3 (1965).
10) M. G. Gunn et al: "Electron Beam Fusion Zone Penetration in 12 mm (1/2 in) Austenitic Stainless Steel", Advances in Welding Processes., 14-16 April (1970).
11) P. J. Konkol et al: "Parameter Study of Electron Beam Welding", W. J., Vol. 50 No. 11 (1971).
12) Y. Arata: "Characteristics of Electron Beam Heat Source and View of Development of Its Welding Technology", J. Japan Welding Society, Vol. 41 No. 11 (1972) (in Japanese)